Experiments Using the Argonne Fragment Mass Analyzer*

C. N. Davids,[a] B. Back,[a] I. G. Bearden,[b] K. Bindra,[a],[c] C. R. Bingham,[d] R. Broda,[b],[e] M. P. Carpenter,[a] W. Chung,[a],[f] P. J. Daly,[b] B. Fornal,[b] Z. W. Grabowski,[b] D. J. Henderson,[a] R. G. Henry,[a] R. V. F. Janssens,[a] T. L. Khoo,[a] T. Lauritsen,[a] Y. Liang,[a] R. H. Mayer,[b] D. M. Moltz,[g] D. Nisius,[b] A. V. Ramayya,[c] J. D. Robertson,[h] F. Scarlassara,[i] F. Soramel,[a],[i] P. Spolaore,[i] K. S. Toth,[j] W. B. Walters[k]

[a]Argonne National Laboratory, Argonne, IL
[b]Purdue University, W. Lafayette, IN
[c]Vanderbilt University, Nashville, TN
[d]University of Tennessee, Knoxville, TN
[e]Institute of Nuclear Physics, Cracow, Poland
[f]University of Notre Dame, South Bend, IN
[g]Lawrence Berkeley Laboratory, Berkeley, CA
[h]University of Kentucky, Lexington, KY
[i]Legnaro National Laboratory, Legnaro, Italy
[j]Oak Ridge National Laboratory, Oak Ridge, TN
[k]University of Maryland, College Park, MD

The Fragment Mass Analyzer (FMA) at the ATLAS accelerator has been operational for about one year. During that period a number of test runs and experiments have been carried out. The test runs have verified that the ion optics of the FMA are essentially as calculated. A brief facility description is followed by recent experimental results.

I. Introduction

The FMA[1,2] is an 8.2-meter long triple-focussing (energy, x, y) recoil mass spectrometer installed at the ATLAS heavy-ion accelerator at Argonne National Laboratory. Figure 1 shows a schematic diagram of the FMA. The FMA separates reaction products from the primary heavy-ion beam and disperses them by M/q at the focal plane. When the FMA is positioned at 0°, the primary beam is stopped on the anode of the first electric dipole, and the two electric dipoles plus the bending magnet constitute an energy-dispersionless mass spectrometer for the reaction products. The two magnetic quadrupole doublets provide geometric focussing and control of M/q dispersion at the focal plane. The FMA has an energy acceptance of ±20%, an M/q acceptance of ±4%, a maximum solid angle of 8 msr, variable mass dispersion, and an M/q resolution of >300:1. The FMA can be positioned at angles between -5° and +45°, as well as at distances from the target variable from 10 - 100 cm in order to accommodate large detector arrays at the target. Figure 2 shows a photograph of the FMA.

The submitted manuscript has been authored by a contractor of the U. S. Government under contract No. W-31-109-ENG-38. Accordingly, the U. S. Government retains a nonexclusive, royalty-free license to publish or reproduce the published form of this contribution, or allow others to do so, for U. S. Government purposes.

II. Ion-Optical Design

The ion optics of the FMA resemble, with some important differences, the optics of the recoil mass spectrometer CAMEL[3] located at the Legnaro National Laboratory in Italy. The CAMEL spectrometer uses the same achromatic combination of electric and magnetic dipoles, but has only one magnetic quadrupole doublet, located at the entrance. The second quadrupole doublet in the FMA allows a variable mass dispersion $(x|\delta_M)$ at the focal plane, as well as providing excellent vertical focussing.

First-order cancellation of the energy dispersion $[(x|\delta_E)=0, (\theta|\delta_E)=0]$ is obtained by separating each electric dipole from the magnetic dipole by a distance of 1200 mm. Here x is the horizontal displacement from the optic axis, θ is the horizontal angle, and δ_E represents the fractional difference from the central particle energy, $(E-E_0)/E_0$. The beam diverges slightly in the horizontal direction while passing through the first electric dipole, so the maximum horizontal angle at the target is determined by the 10-cm gap between the electric dipole plates. Pole edge curvature of the 40° magnet introduces a second-order correction to the optics, and the principal second-order aberration remaining at the focal plane is due to the geometrical coefficient $(x|\theta^2)$. After M/q dispersion occurs in the 40° magnet, the different M/q's diverge as they enter the second electric dipole, with the range of M/q values finally transmitted being limited by the plate gap. The nominal target-to-entrance quadrupole and exit quadrupole-to-focal plane distances are both 30 cm for the FMA.

III. Experimental Equipment

A number of different experimental systems are available for use with the FMA. Some of these have been constructed by University users.

A 38-cm diameter sliding seal scattering chamber is available for use at the target position. It has provision for a target ladder as well as a rotating target wheel used under high beam current conditions. There are two independently-controlled rings for mounting detectors, and one side of the chamber has a 30.5-cm by 30.5-cm opening to accommodate an extension for housing large gas detectors. All variable parameters are equipped with stepping motors, controlled manually or by computer. With this scattering chamber in place, the normal distance between the target and the entrance quadrupole is 30 cm. Vacuum is provided by a 1500 l/s cryopump attached to the side of the chamber.

For prompt gamma-ray experiments, an array of ten Compton-suppressed Ge detectors can be placed around the FMA target position. With the full complement of 10 detectors, the distance between the target and the FMA is 35.6 cm. For these experiments the 38-cm scattering chamber is replaced by a 12.1-cm diameter target chamber containing a Si detector beam monitor, a target ladder driven by a stepping motor, and a device to insert thin carbon foils behind the target. These foils are used to reset the charge state of the reaction products following the emission of de-excitation gamma rays.

A 16-segment neutron detector array is available for use at the FMA target position, normally used in conjunction with the Compton-suppressed Ge detectors. It occupies the region between the small target chamber and the entrance to the FMA, so that neutrons evaporated in the forward direction can be detected. In coincidence measurements the neutron array can be used to provide additional information on the Z of the recoils. The detectors utilize pulse shape to discriminate between neutrons and gamma rays at neutron energies above 1 to 2 MeV, and time-of-flight for lower energies.

At the focal plane a 15-cm horizontal by 5-cm vertical parallel-plate avalanche counter (PPAC) is used to measure x- and y-position, time and energy loss. The PPAC has mylar entrance and exit windows of total thickness 280 $\mu g/cm^2$, and uses isobutane gas at a pressure of 3 Torr. Behind it can be placed other detectors such as Si or Bragg curve detectors, or the recoils can be allowed to proceed into other detector systems. A moving tape collector is available for studies of beta activities. A facility to study nuclear moments is under construction behind the FMA. It consists of an array of tilted foils for polarizing the recoils, and a magnet for beta-NMR measurements. Currently under design is an implantation-decay detection system based on a double-sided Si strip detector with a total of 48 x 48 pixels.

IV. Some Experimental Results

a) Yrast Isomers in ^{151}Yb

Recoil ions have transit times through the FMA in the range 0.5-2 μs, providing an ideal opportunity to study the decays of microsecond isomers at the focal plane[4]. The ^{96}Ru + 255 MeV-^{58}Ni reaction was used to produce fusion products near mass 151, and after passing through the PPAC, were stopped on a catcher foil placed 10 cm behind the focal plane. Delayed gamma-recoil and gamma-gamma coincidences from the stopped recoils were measured between the PPAC and three gamma detectors. Besides transitions resulting from the decay of the known $N = 82$ isomers 2.6 μs ^{150}Er, 0.46 μs ^{151}Tm and 34 ms ^{152}Yb, two yrast isomers with half-lives of 20 ± 1 μs and 2.6 ± 0.7 μs were observed in ^{151}Yb. Figure 3 shows the clean separation of transitions feeding and de-exciting the 2.6 μs isomer, obtained by sorting the mass-selected gamma-gamma coincidence events using appropriate timing conditions. Further work on these isomers is planned, in particular the observation of conversion electrons using a Si detector.

b) Gamma Spectroscopy of Hg Isotopes

The first gamma-ray spectroscopic studies using the array of ten Compton-suppressed Ge detectors around the FMA target position have been conducted. The reactions ^{155}Gd + ^{32}S (160 and 190 MeV) and ^{160}Gd + ^{36}S (157 MeV) were used to produce $^{181-183}Hg$ and $^{190-192}Hg$. The recoil transmissions (see Sec. V) obtained in these runs were 5-10%, with 2 charge states on the focal plane.

The data for the ^{36}S + ^{160}Gd reaction demonstrate the sensitivity of the FMA for weak channels. Figure 4 shows how using the mass resolution of the FMA allows one to pull out the gamma rays from the weakly-produced mass 189 channel.

c) Alpha Decay of Neutron-Deficient Pt Isotopes

Early in the commissioning phase of the FMA an experiment was performed to study the decay of short-lived neutron-deficient platinum α-emitting isotopes produced by bombarding ^{144}Sm by ^{32}S. The Pt recoils traversed the FMA, passed through the PPAC at the focal plane and were implanted into a Si detector placed about 10 cm behind the PPAC. Alpha decay events in the Si detector were counted both during bombardment and beam-off intervals. An electrostatic sweeper was used to prevent the beam from entering the ATLAS accelerator during the beam-off period.

Two different bombarding energies were used: 164 MeV to favor the production of ^{172}Pt and ^{173}Pt, and 200 MeV to favor the production of ^{170}Pt and ^{171}Pt. The half-lives of ^{173}Pt and ^{172}Pt were determined to be 290(60) and 110(20) ms, in agreement with literature values.[5,6] Figure 5 shows a spectrum accumulated during the beam-off period for the 164-MeV run. Not only are the alphas from $^{171,172,173}Pt$ present in the spectrum, but also the alphas from their decay daughters as well. Future experiments will continue this work and extend it to other alpha emitters in this mass region.

V. Operational Properties of the FMA and Future Plans

The primary beam suppression of the FMA is defined as the primary beam intensity at the target divided by the intensity of primary beam particles measured on the focal plane detector. The suppression has been measured using a ^{58}Ni beam on a number of targets with masses between 27 and 197. The values ranged from 10^6 in the former case to 10^{11} for the latter. High primary beam suppression is obtained by using light beams and heavy targets.

The recoil transmission of the FMA is defined as the number of recoils reaching the focal plane divided by the number of recoils produced at the target, and is highly dependent on a number of variables. First is the FMA's geometric acceptance, typically 5 msr. The transmission also depends on the reaction kinematics and the target thickness, because they determine the angular-, energy-, and charge-state distribution for recoils emerging from the target. Finally, the transmission depends on the M/q of the recoil compared to the central M/q. The transmission of a particular recoil species is measured by observing, in singles and in coincidence with recoils at the focal plane, a particular gamma transition at the target position. The highest transmission measured so far is from a ^{58}Ni on ^{64}Ni experiment. Here a transmission of 24% was measured for the 2p2n evaporation product ^{118}Xe. Figure 6 shows the M/q spectrum obtained during that measurement, showing two charge states for M = 118 on the focal plane.

The mass resolution of the FMA is detennined by the beam spot size on target and the angular and energy distributions of the recoils. A circular beam spot size of about 1-mm diameter is used at the FMA target. The highest mass resolution obtained so far with the FMA, 525:1, is shown in Figure 6. In other experiments where the reaction kinematics have been less favorable, mass resolutions of about 350:1 have been obtained.

The FMA has been tested with reactions utilizing both conventional and inverse kinematics. Inverse kinematics has the advantages of high transmission due to forward focussing of the recoils, and high recoil energies which aids in Z-identification. It has the disadvantages of lower primary beam suppression and large gamma-ray Doppler shifts at the target.

At present, development work is proceeding on new configurations of detectors for the focal plane, including highly-segmented Si detectors for implantation studies and a gas ionization chamber for Z-identification.

References

* Work supported by the U.S. Department of Energy, Nuclear Physics Division, under contract W-31-109-ENG-38

1 C. N. Davids and J. D. Larson, Nucl. Instr. and Meth. B40/41, 1224(1989)
2 C. N. Davids *et al.*, Nucl. Instr. and Meth. B70, 358(1992)
3 P. Spolaore *et al.*, Nucl. Instr. and Meth. A238, 381(1985)
4 D. Nisius *et al.*, submitted to Physical Review C
5 V. S. Shirley, Nucl. Data Sheets 54, 589(1988)
6 W. Gonqing, Nucl. Data Sheets 51, 577(1987)

Figure Captions

1. Schematic diagram of the Fragment Mass Analyzer

2. Photograph of the FMA. The primary beam is incident from the lower left.

3. Gamma rays observed at the FMA focal plane from the decay of high-spin isomers in ^{151}Yb.

4. Results from the $^{36}S + ^{160}Gd$ reaction. a) Mass projection showing the low yield of mass 189. b) A portion of the total γ-projection of the recoil-γγ matrix. Gamma rays from all masses observed in recoil coincidence are present, and the strongest transition in ^{189}Hg at 403 keV is identified. c) A portion of the mass 189-gated γ-projection of the recoil-γ-γ matrix.

5. Alpha-particle spectrum of recoils implanted into a Si detector behind the FMA focal plane, accumulated during the beam-off interval.

6. M/q spectrum at the FMA focal plane from the $^{58}Ni + ^{64}Ni$ reaction at 215 MeV.

ANL-P-20,406

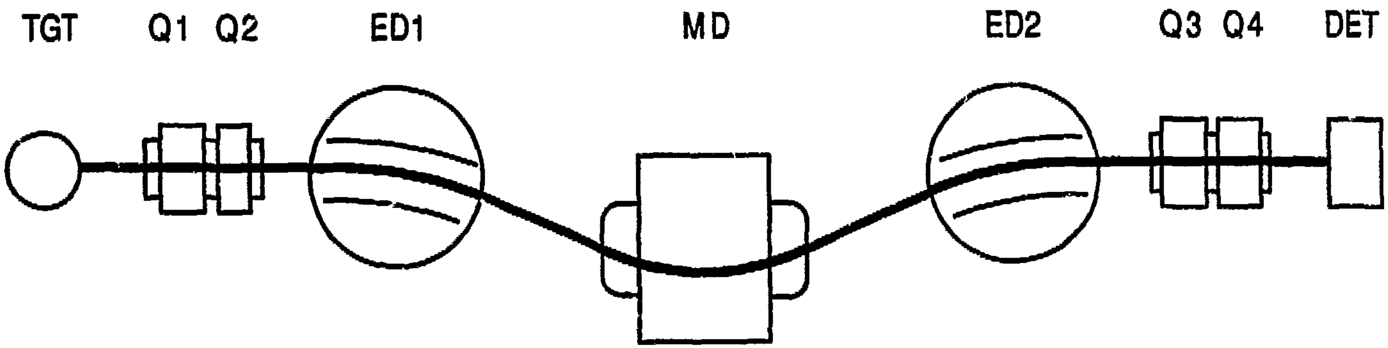

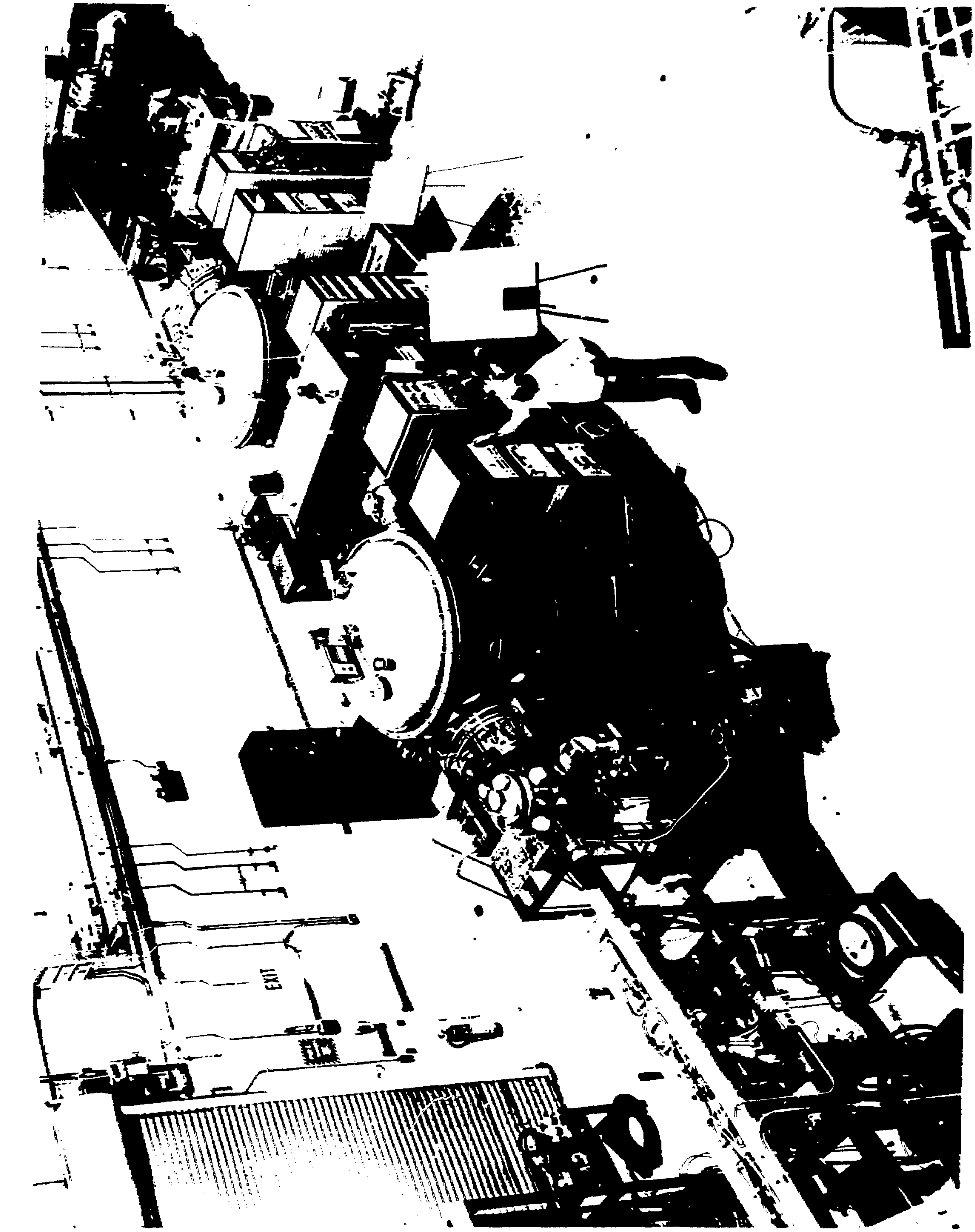
EXIT

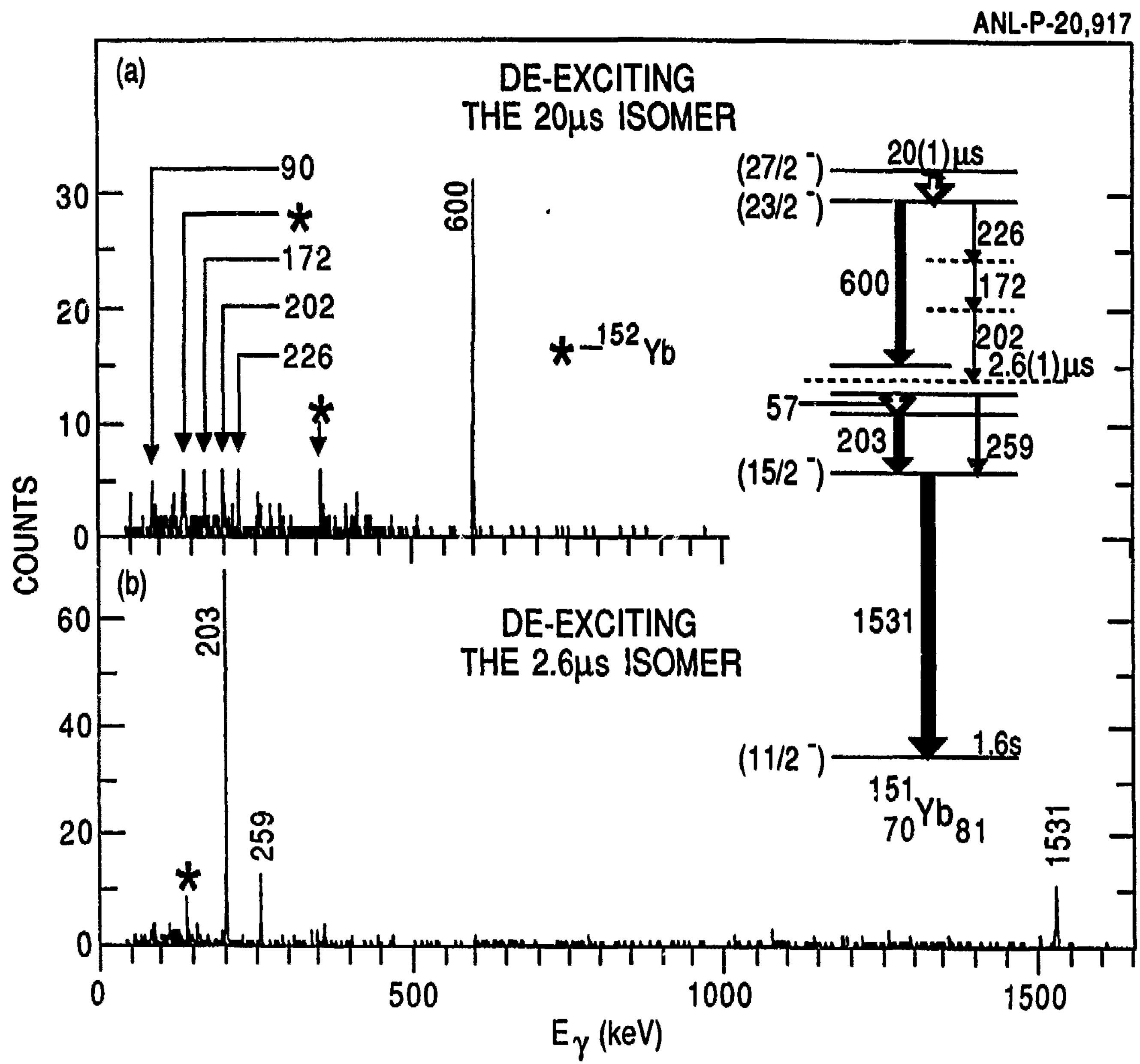
ANL-P-20,917
(a)
DE-EXCITING
THE 20μs ISOMER
90
172
202
226
600
*
*–152Yb
(27/2⁻)
(23/2⁻)
20(1)μs
226
172
202
2.6(1)μs
600
57
203
259
(15/2⁻)
1531
(11/2⁻)
1.6s
151 70 Yb 81
(b)
DE-EXCITING
THE 2.6μs ISOMER
203
259
1531
COUNTS
Eγ (keV)
0
10
20
30
40
60
500
1000
1500

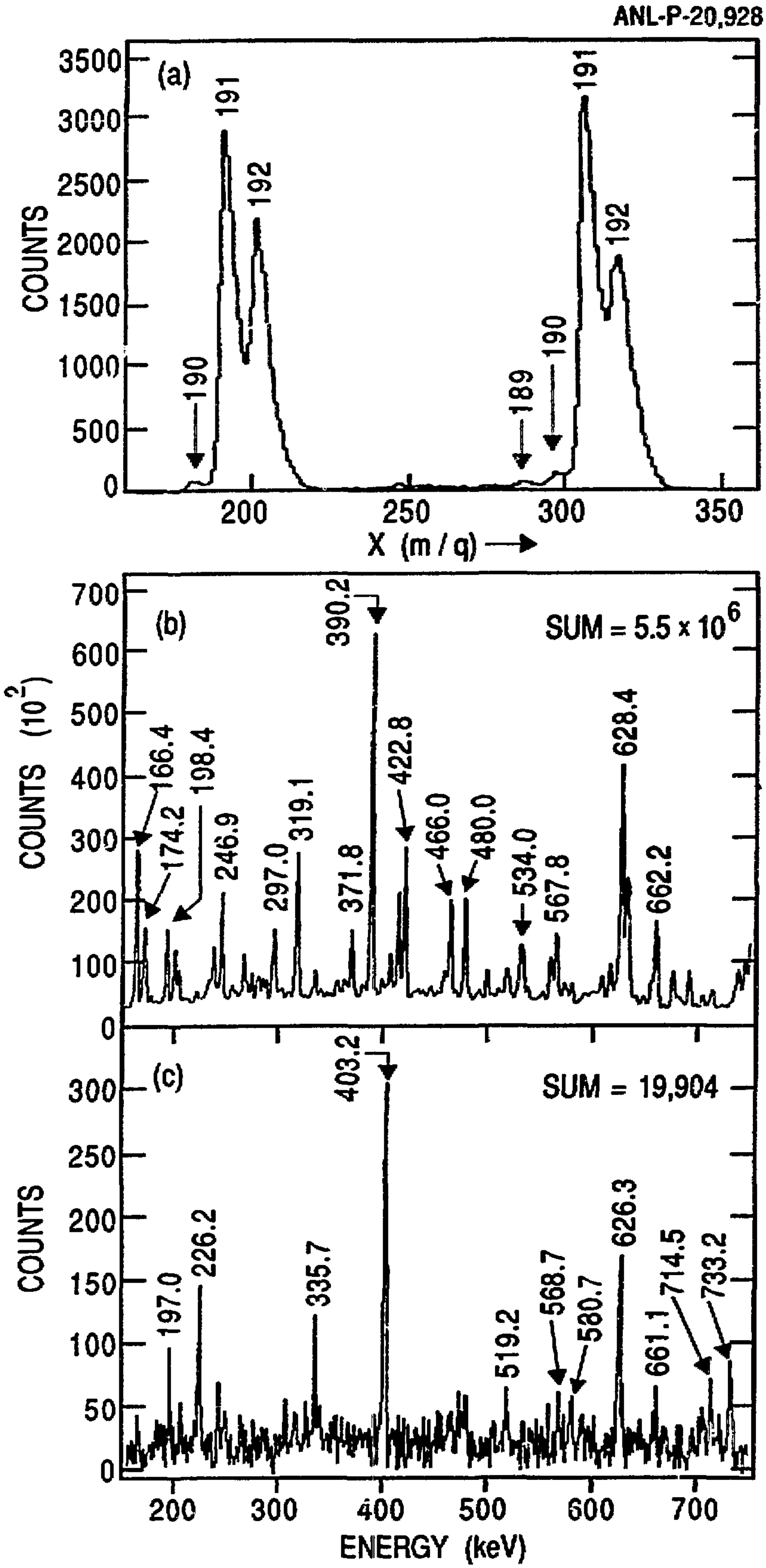

ANL-P-20,928
(a)
COUNTS
3500
3000
2500
2000
1500
1000
500
0
190
191
192
189
190
191
192
200
250
300
350
X (m / q)
(b)
COUNTS (10^2)
700
600
500
400
300
200
100
0
SUM = 5.5 x 10^6
166.4
174.2
198.4
246.9
297.0
319.1
371.8
390.2
422.8
466.0
480.0
534.0
567.8
628.4
662.2
(c)
COUNTS
300
250
200
150
100
50
0
SUM = 19,904
197.0
226.2
335.7
403.2
519.2
568.7
580.7
626.3
661.1
714.5
733.2
200
300
400
500
600
700
ENERGY (keV)

ANL-P-20,727

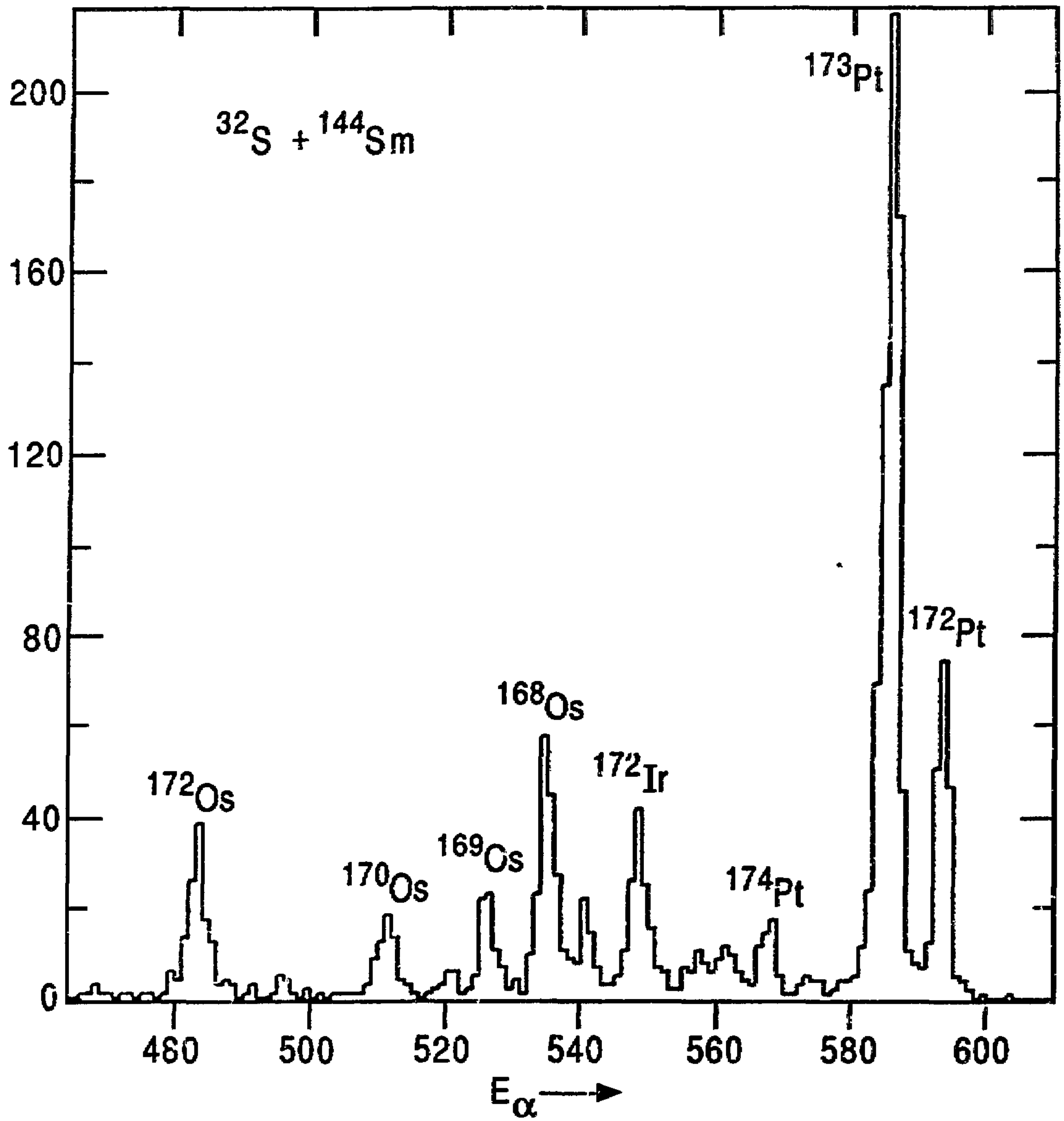

^{32}S + ^{144}Sm
^{173}Pt
^{172}Pt
^{168}Os
^{172}Ir
^{172}Os
^{169}Os
^{170}Os
^{174}Pt
0
40
80
120
160
200
480
500
520
540
560
580
600
E$_\alpha$ →

ANL-P-20,722

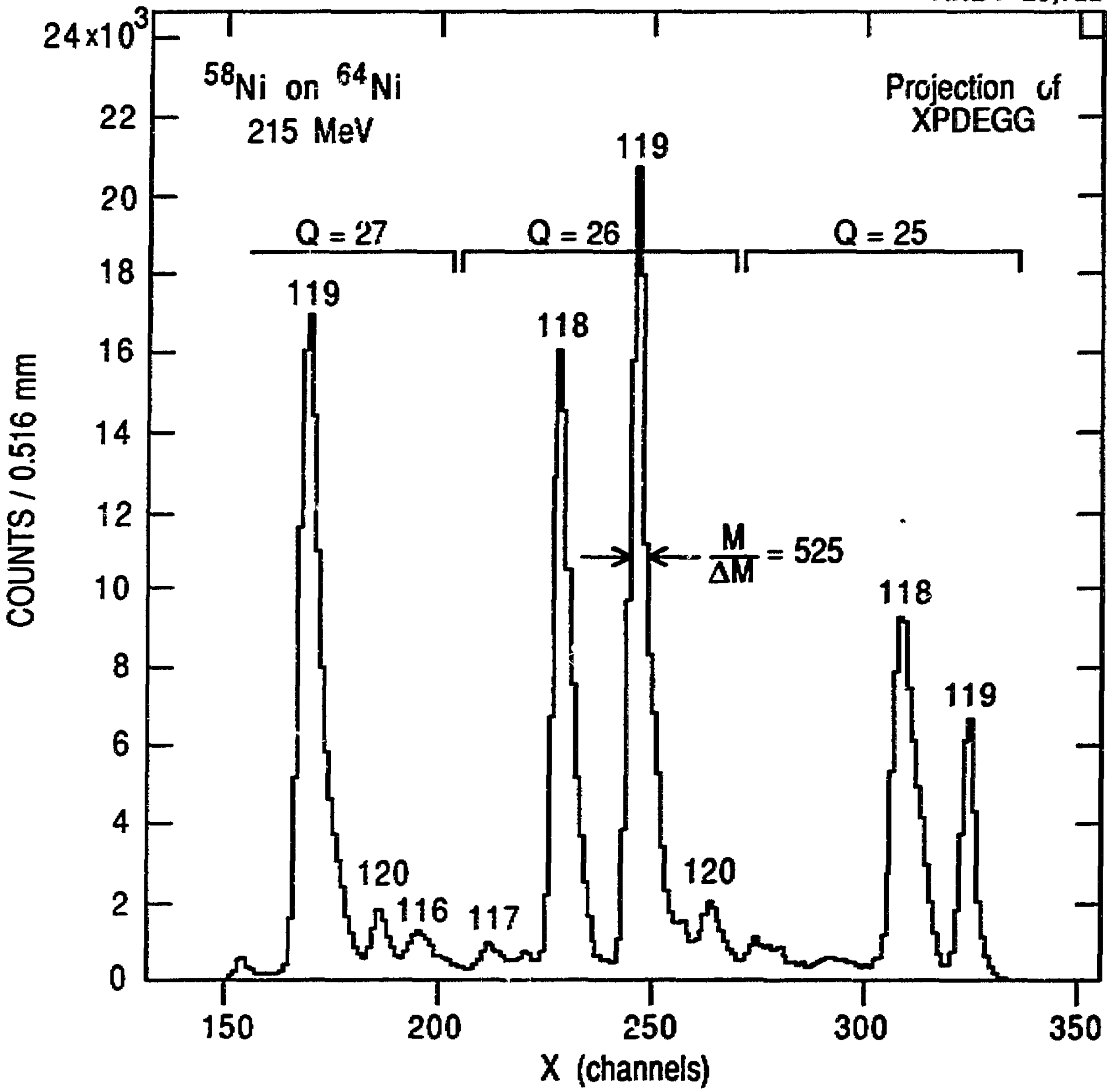

24x10^3
22
20
18
16
14
12
10
8
6
4
2
0
COUNTS / 0.516 mm
58Ni on 64Ni
215 MeV
Projection of
XPDEGG
Q = 27
Q = 26
Q = 25
119
118
119
120
116
117
120
118
119
M/ΔM = 525
150
200
250
300
350
X (channels)